Electrochimica Acta 55 (2010) 2978–2982

Contents lists available at ScienceDirect

Electrochimica Acta

journal homepage: www.elsevier.com/locate/electacta

Preparation and electrochemical performance of $Li_4Ti_5O_{12}$/carbon/carbon nano-tubes for lithium ion battery

Xing Li [a,b], Meizhen Qu [a], Yongjian Huai [a,b], Zuolong Yu [a,*]

[a] Chengdu Institute of Organic Chemistry, Chinese Academy of Sciences, Chengdu 610041, China
[b] Graduate University of the Chinese Academy of Sciences, Beijing 100049, China

ARTICLE INFO

Article history:
Received 24 October 2009
Received in revised form 4 January 2010
Accepted 5 January 2010
Available online 15 January 2010

Keywords:
Lithium ion battery
$Li_4Ti_5O_{12}$/C/CNTs composite
$Li_4Ti_5O_{12}$/C composite
Conductive network
Rate capability

ABSTRACT

A $Li_4Ti_5O_{12}$/carbon/carbon nano-tubes ($Li_4Ti_5O_{12}$/C/CNTs) composite was synthesized by using a solid-state method. For comparison, a $Li_4Ti_5O_{12}$/carbon ($Li_4Ti_5O_{12}$/C) composite and a pristine $Li_4Ti_5O_{12}$ were also synthesized in the present study. The microstructure and morphology of the prepared samples are characterized by XRD and SEM. Electrochemical properties of the samples are evaluated by using galvanostatic discharge/charge tests and AC impedance spectroscopy. The results reveal that the $Li_4Ti_5O_{12}$/C/CNTs composite exhibits the best rate capability and cycling stability among the samples of $Li_4Ti_5O_{12}$, $Li_4Ti_5O_{12}$/C and $Li_4Ti_5O_{12}$/C/CNTs. At the charge–discharge rate of 0.5 C, 5.0 C and 10.0 C, its discharge capacities were 163 mAh/g, 148 mAh/g and 143 mAh/g, respectively. After 100 cycles at 5.0 C, it remained at 146 mAh/g.

1. Introduction

Lithium ion batteries have been widely applied as power sources for electronic devices such as cameras, mobile phones, computers and other related devices. Recently, lithium ion batteries have also attracted attention as electric sources for electric and hybrid electric vehicles (EVs and HEVs), respectively [1]. In fact, the development of lithium ion batteries with high power and high energy density is key to their successful application in EVs and HEVs [2]. For this purpose, new electrode materials exhibiting high charge/discharge current rates are urgently requested. The spinel lithium titanate ($Li_4Ti_5O_{12}$) has been demonstrated as a potential candidate for the anode electrode material in high power Li-ion batteries as well as hybrid super capacitors [3–11] because it has some unique characteristics as compared with carbon based anode materials. It has good structural stability with an almost negligible volume change during the Li^+ insertion and extraction processes, which suggests virtually unlimited cycle life. It features a flat operating voltage of about 1.5 V versus lithium, which is higher than the reduction potential of most electrolyte solvents. These characteristics indicate that $Li_4Ti_5O_{12}$ is advantageous as an anode for use in lithium ion batteries with safety, long life and reliability.

Despite these mentioned advantages, however, $Li_4Ti_5O_{12}$ suffers from the problem of poor rate capability mainly due to its low electronic conductivity. Several methods have been utilized to improve the electronic conductivity of $Li_4Ti_5O_{12}$. These include synthesizing $Li_4Ti_5O_{12}$ with small particle sizes [12,13], heating pure $Li_4Ti_5O_{12}$ under a reducing atmosphere [14], doping $Li_4Ti_5O_{12}$ with aliovalent metal ions [15–21] and forming a composite of $Li_4Ti_5O_{12}$ and a conductive second phase such as Ag, C and polyacene [22–27]. According to the literatures, synthesizing a composite of $Li_4Ti_5O_{12}$ and a conductive second phase is a good way to improve the electronic conductivity for this can take part in controlling particle growth and can uniformly coat on the surface of the $Li_4Ti_5O_{12}$ material, which are favorable to the transfer of the electron. However, this method cannot efficiently improve the electronic conductivity of $Li_4Ti_5O_{12}$. This is because that the conductive second phases are generally nano-size particles, which result in the composites of $Li_4Ti_5O_{12}$/conductive second phases still make no actual contact with each other in the electrode. In the present work, we found that a composite of $Li_4Ti_5O_{12}$/carbon/carbon nanotubes ($Li_4Ti_5O_{12}$/C/CNTs) had better electrochemical performance than a composite of $Li_4Ti_5O_{12}$/carbon ($Li_4Ti_5O_{12}$/C). We believed this is because that the CNTs can act like bridges, which connect the isolated particles of $Li_4Ti_5O_{12}$/C, resulting in the composite of $Li_4Ti_5O_{12}$/C/CNTs has better electronic conductivity than the composite of $Li_4Ti_5O_{12}$/C. For comparison, pristine $Li_4Ti_5O_{12}$ was also investigated.

2. Experimental

$Li_4Ti_5O_{12}$ was prepared from TiO_2 (anatase structure) and Li_2CO_3 by using a solid-state method. The starting materials, TiO_2

* Corresponding author. Tel.: +86 28 85229790; fax: +86 28 85242280.
E-mail addresses: yzuolong@163.com, yu.zuolong@yahoo.com (Z. Yu).

0013-4686/$ – see front matter © 2010 Elsevier Ltd. All rights reserved.
doi:10.1016/j.electacta.2010.01.015

and Li_2CO_3 in a Li:Ti molar ratio of 4:5 were mixed in acetone and ball-milled for 24 h. The obtained binary precursor slurry was treated at 80 °C, and became dried powder. The dried powder was then calcinated at 800 °C for 12 h in Ar atmosphere. The $Li_4Ti_5O_{12}$/C was also prepared by using a similar solid-state method as mentioned above. In this case, however, it was prepared from a ternary precursor mixture of TiO_2, Li_2CO_3 and pitch. The $Li_4Ti_5O_{12}$/C/CNTs was prepared with TiO_2, Li_2CO_3, pitch and CNTs. Firstly, TiO_2, Li_2CO_3 and pitch were mixed in acetone and ball-milled for 24 h to obtain a homogeneous mixed slurry. CNTs were dispersed in acetone with sufficient ultrasonication to form a uniform slurry. The obtained two slurries were then mixed together and treated at 80 °C to become dried powder. Finally, the dried powder was calcinated at 800 °C for 12 h in Ar atmosphere. The CNTs are multi-wall CNTs with a diameter and length of about 20–30 nm and 1–2 μm respectively, produced from Chengdu Organic Chemicals Co. Ltd.

The crystal structures of the samples were characterized by X-ray powder diffraction (XRD) measurement using the Philips X' Pert Pro MPD DY1219 with a Cu K_α radiation source. Particle morphologies of the samples were observed by scanning electronic microscopy (SEM FEI INSPECT-F). The amount of C in $Li_4Ti_5O_{12}$/C composite and C and CNTs in $Li_4Ti_5O_{12}$/C/CNTs composite were measured by thermogravimetry (TG) and differential thermal analysis (DTA) method, using HENVEN HCT-1, with scanning rate of 10 °C in air atmosphere from 25 °C to 800 °C. Specific surface areas of the samples were determined through nitrogen adsorption/desorption at −196 °C using a Builder SSA-4200 apparatus.

The electrochemical characterizations were measured by means of two-electrode coin-type half cells, which consist of $Li_4Ti_5O_{12}$-, $Li_4Ti_5O_{12}$/C- or $Li_4Ti_5O_{12}$/C/CNTs-based positive electrode (92 wt.% active material, 3 wt.% acetylene black and 5 wt.% LA-132 binder), a Celgard 2400 separator, and a lithium foil as negative electrode. The active mass and electrode thickness of the positive electrode are about 4.5 mg and 50 μm, respectively. The electrolyte was 1 M $LiPF_6$/EC:DEC:DMC (1:1:1 in volume). The cells were assembled in a glove box filled with high purity argon gas. Galvanostatic discharge–charge measurements were performed at constant cut-off voltages of 1–3 V at room temperature (25 °C). The AC impedance spectrum was measured by using a Solatron 1260 Impedance Analyzer in the frequency range 10^{-2}–10^6 Hz.

3. Results and discussion

X-ray diffraction patterns of the samples are shown in Fig. 1. From Fig. 1, it can be observed that the main phases of all investigated samples are $Li_4Ti_5O_{12}$ with a cubic spinel structure, which suggests that the addition of pitch or pitch and CNTs in the precursor does not influence the formation of spinel $Li_4Ti_5O_{12}$ during heat-treatment. Furthermore, Fig. 1 shows that the patterns of the $Li_4Ti_5O_{12}$, $Li_4Ti_5O_{12}$/C and $Li_4Ti_5O_{12}$/C/CNTs are similar, except for a weak peak in the curve of $Li_4Ti_5O_{12}$/C/CNTs at 26°(2θ) due to the CNTs in the composite.

Fig. 2 shows the SEM pictures of the $Li_4Ti_5O_{12}$, $Li_4Ti_5O_{12}$/C and $Li_4Ti_5O_{12}$/C/CNTs samples. Image A is the $Li_4Ti_5O_{12}$ sample, image B is the $Li_4Ti_5O_{12}$/C sample and image C is the $Li_4Ti_5O_{12}$/C/CNTs sample. There, it can be observed that the particles of $Li_4Ti_5O_{12}$/C and $Li_4Ti_5O_{12}$/C/CNTs have relatively less agglomerations while the particle of $Li_4Ti_5O_{12}$ form larger agglomerations. In the composite of $Li_4Ti_5O_{12}$/C/CNTs, it can be seen that the CNTs are well dispersed among $Li_4Ti_5O_{12}$/C particles. Furthermore, as is shown in the close-up SEM images of A, B and C, the particle surface of $Li_4Ti_5O_{12}$ is smooth, whereas the $Li_4Ti_5O_{12}$/C and $Li_4Ti_5O_{12}$/C/CNTs composites have a rougher surface, which should be ascribed to the carbon derived from pitch during heat-treatment.

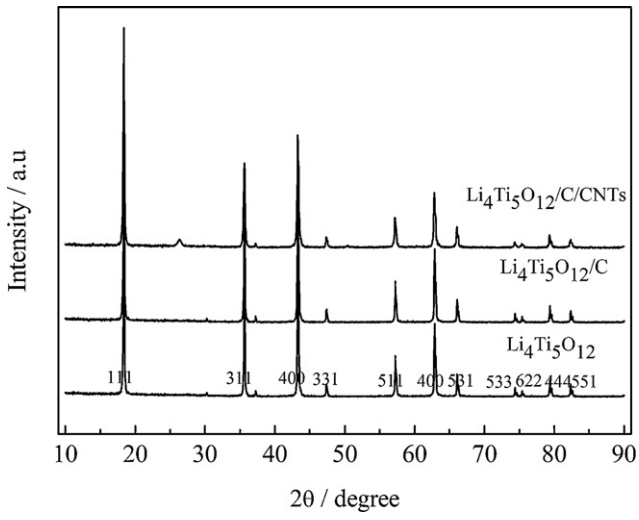

Fig. 1. X-ray diffraction patterns of synthesized $Li_4Ti_5O_{12}$, $Li_4Ti_5O_{12}$/C and $Li_4Ti_5O_{12}$/C/CNTs samples.

The content of C in the composite of $Li_4Ti_5O_{12}$/C and the content of C and CNTs in the composite of $Li_4Ti_5O_{12}$/C/CNTs were measured by a TG-DTA method, as shown in Figs. 3 and 4 respectively. Fig. 3 shows that there is a single exothermic peak at about 450 °C and the content of C in the composite of $Li_4Ti_5O_{12}$/C is about 6% by weight. Fig. 4 exhibits that there are two exothermic peaks at about 450 °C and 650 °C respectively and the total content of C and CNTs in the composite of $Li_4Ti_5O_{12}$/C/CNTs is also about 6% by weight. Furthermore, as is shown in Fig. 4, the weight ratio of C and CNTs in the composite of $Li_4Ti_5O_{12}$/C/CNTs is about 1:1. Table 1 shows the BET surface areas of the $Li_4Ti_5O_{12}$, $Li_4Ti_5O_{12}$/C, $Li_4Ti_5O_{12}$/C/CNTs, CNTs and C. There, it can be observed that the BET surface areas of the $Li_4Ti_5O_{12}$, $Li_4Ti_5O_{12}$/C, $Li_4Ti_5O_{12}$/C/CNTs, CNTs and C are 22.8 m^2/g, 31.5 m^2/g, 36.4 m^2/g, 128 m^2/g and 0.8 m^2/g, respectively. Since the percentage of C in the composite of $Li_4Ti_5O_{12}$/C amounts to 6% and the BET surface area of that $Li_4Ti_5O_{12}$/C composite is comprised of 94% $Li_4Ti_5O_{12}$ and 6% C, and the BET surface area of $Li_4Ti_5O_{12}$ in the composite of $Li_4Ti_5O_{12}$/C is 33.46 m^2/g. The above calculation process can be summarized as the following formula:

$$0.94 \times S_{\mathrm{LiTiO}} + 0.06 \times S_{\mathrm{carbon}} = S_{\mathrm{LiTiO/C}}$$

According to the above mentioned method, the calculation process of the BET surface area of $Li_4Ti_5O_{12}$ in the composite of $Li_4Ti_5O_{12}$/C/CNTs can be summarized as the following formula:

$$0.94 \times S_{\mathrm{LiTiO}} + 0.03 \times S_{\mathrm{carbon}} + 0.03 \times S_{\mathrm{CNTs}} = S_{\mathrm{LiTiO/C/CNTs}}$$

From the above formula, it can calculate that the BET surface area of $Li_4Ti_5O_{12}$ in the composite of $Li_4Ti_5O_{12}$/C/CNTs is 34.61 m^2/g. These results indicate that the BET surface areas of $Li_4Ti_5O_{12}$ in the composite of $Li_4Ti_5O_{12}$/C and $Li_4Ti_5O_{12}$/C/CNTs are obviously larger than that of the $Li_4Ti_5O_{12}$ (22.8 m^2/g) without the addition of pitch or pitch and CNTs. It is well known that smaller particle sizes can be obtained by adding carbon to the precursor because this can control particle growth [28] during heat-treatment. The above results indicate that the addition of pitch or pitch and CNTs to the precursor hinders particle agglomeration and growth during the calcination process, resulting in smaller particle sizes.

Fig. 5 shows the AC impedance spectra of the $Li_4Ti_5O_{12}$, $Li_4Ti_5O_{12}$/C and $Li_4Ti_5O_{12}$/C/CNTs electrodes, which were measured at the stable voltage of 1.55 V, respectively. AC impedance spectra are fitted using an equivalent circuit. In this equivalent circuit, R_s and R_{ct} are the solution resistance and charge-transfer resistance, respectively. CPE is placed to represent the double layer

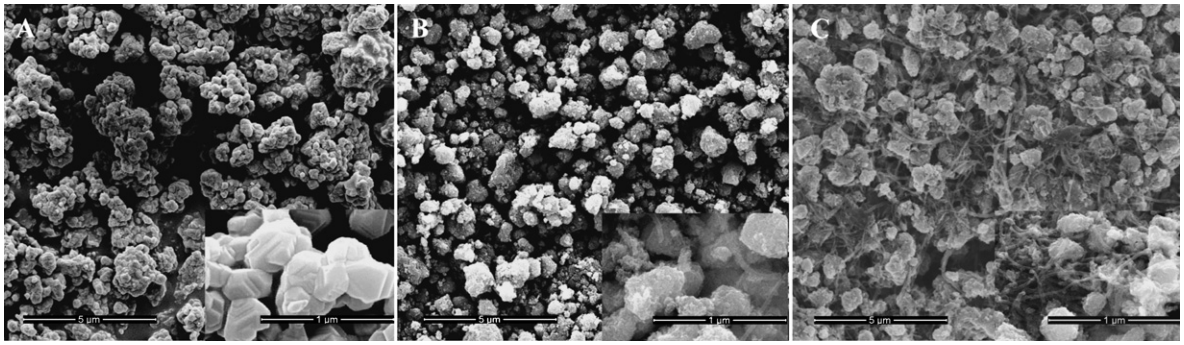

Fig. 2. SEM pictures of $Li_4Ti_5O_{12}$, $Li_4Ti_5O_{12}$/C and $Li_4Ti_5O_{12}$/C/CNTs samples.

Table 1
BET surface areas of the $Li_4Ti_5O_{12}$, $Li_4Ti_5O_{12}$/C, $Li_4Ti_5O_{12}$/C/CNTs, CNTs and C.

	$Li_4Ti_5O_{12}$	$Li_4Ti_5O_{12}$/C	$Li_4Ti_5O_{12}$/C/CNTs	CNTs	C
BET surface area (m^2/g)	22.8	31.5	36.4	128	0.8

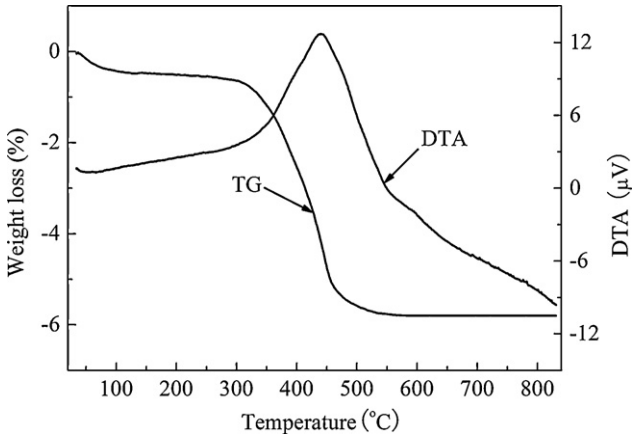

Fig. 3. TG–DTA curves of the $Li_4Ti_5O_{12}$/C composite.

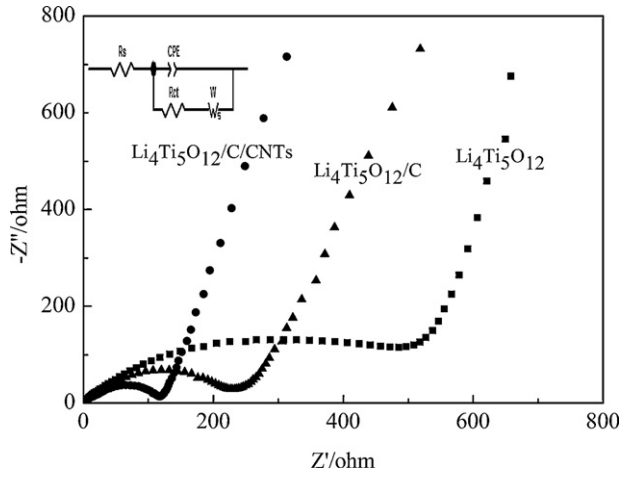

Fig. 5. AC impedance spectra of the $Li_4Ti_5O_{12}$, $Li_4Ti_5O_{12}$/C and $Li_4Ti_5O_{12}$/C/CNTs electrodes at the voltage of 1.55 V.

capacitance and passivation film capacitance. *W* represents the Warburg impedance [29,30]. The parameters of the equivalent circuit are recorded in Table 2.

From Table 2, it can be observed that the exchange current densities ($i^0 = RT/nFR_{ct}$) [31] of $Li_4Ti_5O_{12}$/C and $Li_4Ti_5O_{12}$/C/CNTs cell are higher than the $Li_4Ti_5O_{12}$ cell, and the $Li_4Ti_5O_{12}$/C/CNTs cell has the biggest exchange current density. Furthermore, the $Li_4Ti_5O_{12}$/C and $Li_4Ti_5O_{12}$/C/CNTs electrodes exhibited much lower charge-transfer resistance than that of the $Li_4Ti_5O_{12}$ electrode, and the $Li_4Ti_5O_{12}$/C/CNTs electrode shows the lowest charge-transfer resistance. $Li_4Ti_5O_{12}$/C and $Li_4Ti_5O_{12}$/C/CNTs have higher exchange current densities and lower charge-transfer resistance than $Li_4Ti_5O_{12}$ could be attributed to two reasons: (1) the addition of pitch or pitch and CNTs to the precursor hinders particle agglomeration and growth during the calcination process, resulting in smaller particle sizes, which reduces the distance for lithium ion diffusion while providing a higher electrode/electrolyte contact surface area. Therefore, a better electronic conductivity was achieved. (2) The coating C (derived from pitch) and CNTs are good electron conductive materials, coating on or locating among the $Li_4Ti_5O_{12}$ particles, which are favorable to the electrons transfers. Therefore, they also improve the electronic conductivity. $Li_4Ti_5O_{12}$/C/CNTs has higher exchange current density and lower

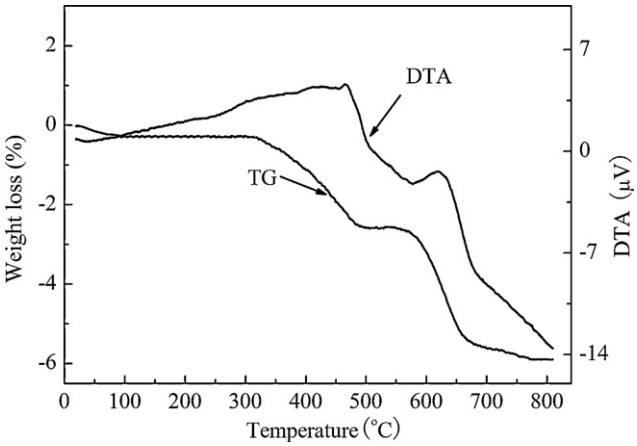

Fig. 4. TG–DTA curves of the $Li_4Ti_5O_{12}$/C/CNTs composite.

Table 2
Impedance parameters of the $Li_4Ti_5O_{12}$, $Li_4Ti_5O_{12}$/C and $Li_4Ti_5O_{12}$/C/CNTs electrodes.

Sample	R_s (Ω)	R_{ct} (Ω)	W ($S^{1/2}$ cm^{-2})	i^0 (mA/cm^2)
$Li_4Ti_5O_{12}$	3.31	203.86	0.00514	0.126
$Li_4Ti_5O_{12}$/C	2.90	155.28	0.00356	0.165
$Li_4Ti_5O_{12}$/C/CNTs	2.42	68.83	0.00172	0.372

charge-transfer resistance than $Li_4Ti_5O_{12}$/C could be ascribed to the following reason: as we know, C is a good electric conductor that uniformly coated on the surface of $Li_4Ti_5O_{12}$ particles, which is favorable to improve the electronic conductivity, however, as shown in the SEM image (image B), it can be seen that C is nano-size particle, might resulting in the composite of $Li_4Ti_5O_{12}$/C still make no actual contact with each other in the electrode, which cannot efficiently improve the electronic conductivity of $Li_4Ti_5O_{12}$. In the composition of $Li_4Ti_5O_{12}$/C/CNTs, as CNTs can act like bridges, connecting the isolated $Li_4Ti_5O_{12}$/C particle and giving rise to valid conductive network in the electrode, which result in the $Li_4Ti_5O_{12}$/C/CNTs has higher exchange current density and lower charge-transfer resistance than that of the $Li_4Ti_5O_{12}$/C.

Fig. 6 shows the cyclic performances of the $Li_4Ti_5O_{12}$, $Li_4Ti_5O_{12}$/C and $Li_4Ti_5O_{12}$/C/CNTs samples at different rates from 0.5 C, 1.0 C, 3.0 C, 5.0 C to 10.0 C. The charge–discharge processes of the samples were taken for 5 cycles at 0.5 C, 1.0 C, 3.0 C, 5.0 C and 10.0 C respectively. As shown in Fig. 5, the discharge capacity gradually decreased with the rate increase for all the samples. However, the $Li_4Ti_5O_{12}$/C/CNTs and $Li_4Ti_5O_{12}$/C samples manifested a higher reversible capacity than the $Li_4Ti_5O_{12}$ sample, especially at high discharge rates. For example, at 5.0 C and at 10.0 C, the capacity of the $Li_4Ti_5O_{12}$/C/CNTs and $Li_4Ti_5O_{12}$/C samples remained 148 mAh/g, 143 mAh/g and 132 mAh/g, 121 mAh/g respectively, while the capacity of the $Li_4Ti_5O_{12}$ sample remained only 100 mAh/g and 74 mAh/g at the same rates. Furthermore, in all the samples, the $Li_4Ti_5O_{12}$/C/CNTs sample exhibited the highest reversible capacity. These results indicate that $Li_4Ti_5O_{12}$/C/CNTs composite exhibits the best rate capability among the samples of $Li_4Ti_5O_{12}$, $Li_4Ti_5O_{12}$/C and $Li_4Ti_5O_{12}$/C/CNTs.

Fig. 7 shows the charge–discharge curves of the $Li_4Ti_5O_{12}$, $Li_4Ti_5O_{12}$/C and $Li_4Ti_5O_{12}$/C/CNTs electrodes at the rate of 10 C. There, it can be seen that $Li_4Ti_5O_{12}$/C and $Li_4Ti_5O_{12}$/C/CNTs have similar charge–discharge plateaus as compared with the $Li_4Ti_5O_{12}$, which indicates that the addition of C or C and CNTs did not affect the electrochemical reaction process of $Li_4Ti_5O_{12}$. Furthermore, the margins between the charge and discharge plateau potentials of $Li_4Ti_5O_{12}$/C/CNTs and $Li_4Ti_5O_{12}$/C are obviously smaller than in the case of $Li_4Ti_5O_{12}$, and the $Li_4Ti_5O_{12}$/C/CNTs has the smallest margin, which means that the polarization of $Li_4Ti_5O_{12}$/C/CNTs and $Li_4Ti_5O_{12}$/C are lower than that of $Li_4Ti_5O_{12}$, and the $Li_4Ti_5O_{12}$/C/CNTs has the smallest polarization.

For evaluating the cycling stability of the $Li_4Ti_5O_{12}$/C/CNTs sample, it was further charge-discharged at a current rate of 5.0 C for another 100 cycles after the 25 cycles electrochemical tests performed at 0.5 C, 1.0 C, 3.0 C, 5.0 C and 10.0 C. This is shown in Fig. 8. It can be observed that the $Li_4Ti_5O_{12}$/C/CNTs sample shows a stable cycle life. The discharge capacity of the sample was 148 mAh/g, and even after 100 charge–discharge cycles, its capacity still remained at 146 mAh/g. Furthermore, as is shown in Fig. 8, the charge and discharge efficiency remained almost at 100%.

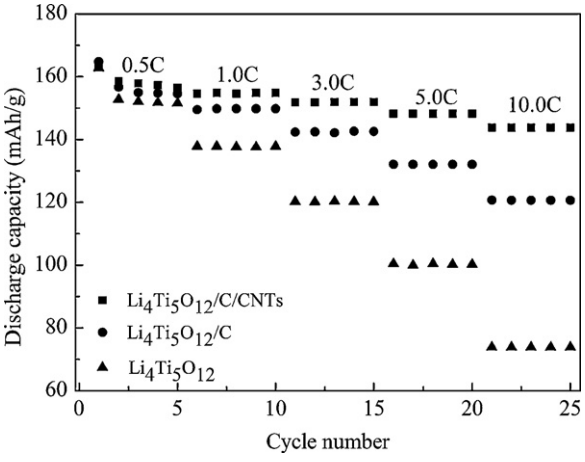

Fig. 6. Cyclic performances of the $Li_4Ti_5O_{12}$, $Li_4Ti_5O_{12}$/C and $Li_4Ti_5O_{12}$/C/CNTs samples at different rates: 1st–5th cycles at 0.5 C, 6th–10th at 1.0 C, 11th–15th at 3.0 C, 16th–20th at 5.0 C, 21th–25th at 10.0 C.

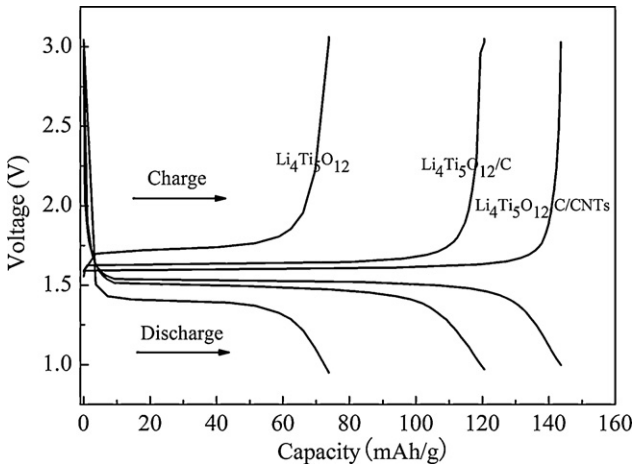

Fig. 7. Charge and discharge curves of the $Li_4Ti_5O_{12}$, $Li_4Ti_5O_{12}$/C and $Li_4Ti_5O_{12}$/C/CNTs electrodes at the rate of 10 C.

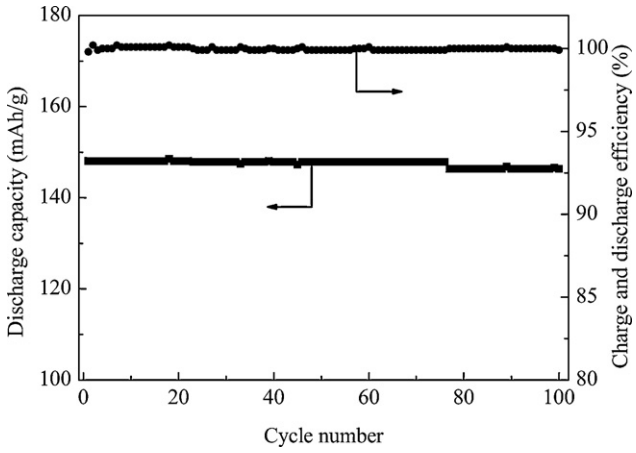

Fig. 8. Cyclic performance of the $Li_4Ti_5O_{12}$/C/CNTs sample at 5.0 C.

4. Conclusions

The $Li_4Ti_5O_{12}$/C/CNTs composite was synthesized and its electrochemical characteristics were investigated in the present study. For comparison, $Li_4Ti_5O_{12}$/C and $Li_4Ti_5O_{12}$ were also investigated. The results show that $Li_4Ti_5O_{12}$/C composite has better electrochemical performances than $Li_4Ti_5O_{12}$, however, $Li_4Ti_5O_{12}$/C/CNTs composite exhibits the best electrochemical performances among the samples of $Li_4Ti_5O_{12}$, $Li_4Ti_5O_{12}$/C and $Li_4Ti_5O_{12}$/C/CNTs. This indicates that although forming a composite of $Li_4Ti_5O_{12}$ and a conductive second phase C could improve the rate capability and cycling stability of $Li_4Ti_5O_{12}$ through controlling particle growth and improving electronic conductivity, the effect was not resultful. It should be attributed to that the C coating on the surface of $Li_4Ti_5O_{12}$ is generally nano-size particle, which might make the composite of $Li_4Ti_5O_{12}$/C still make no actual contact with each other in the electrode. Therefore, it cannot efficiently improve the electronic conductivity of $Li_4Ti_5O_{12}$. In the composite

of $Li_4Ti_5O_{12}$/C/CNTs, however, as CNTs can act like bridges, connecting the isolated $Li_4Ti_5O_{12}$/C particle and giving rise to valid conductive networks in the electrode, resulting in better electronic conductivity, which makes $Li_4Ti_5O_{12}$/C/CNTs composite have better rate capability and cycling stability than that of $Li_4Ti_5O_{12}$/C composite.

Acknowledgements

This work was carried out with financial support from Ministry of Science and Technology of the People's Republic of China (No. 2006CB932703) and Key Item of knowledge Innovation Project of Chinese Academy of Science (No. KJCX2-YW-M01).

References

[1] R.F. Nelson, J. Power Sources 91 (2000) 2.
[2] C. Jiang, E. Hosono, H. Zhou, Nanotoday 1 (2006) 28.
[3] K.M. Colbow, J.R. Dahn, R.R. Haering, J. Power Sources 26 (1989) 397.
[4] K. Zaghib, M. Armand, M. Gauthier, J. Electrochem. Soc. 145 (1998) 3135.
[5] T. Ohzuku, Y. Iwakoshi, K. Sawai, J. Electrochem. Soc. 140 (1993) 2490.
[6] K. Zaghib, M. Simoneau, M. Armand, M. Gauthier, J. Power Sources 81–82 (1999) 300.
[7] A. Guerfi, S. Sevigny, M. Lagace, P. Hovington, K. Kinoshita, K. Zaghib, J. Power Sources 119–121 (2003) 88.
[8] S. Scharner, W. Weppner, P. Schmid-Beurmann, J. Electrochem. Soc. 146 (1999) 857.
[9] M.M. Thackeray, P.J. Johnson, L.A. De Picciott, et al., Mater. Res. Bull. 19 (1984) 179.
[10] T. Ohzuku, A. Ueda, N. Yamamoto, J. Electrochem. Soc. 142 (1995) 1431.
[11] D. Peramunage, K.M. Abraham, J. Electrochem. Soc. 145 (1998) 2609.
[12] A. Guerfi, S. Sevigny, M. Lagace, P. Hovington, K. Kinoshita, K. Zaghib, J. Power Sources 119–121 (2003) 88.
[13] K.N. Jung, S. Pyun, S.W. Kim, J. Power Sources 119–121 (2003) 637.
[14] J. Wolfenstine, U. Lee, J.L. Allen, J. Power Sources 154 (2006) 287.
[15] D.T. Liu, C.Y. Quyang, J. Shu, J. Jiang, Z.X. Wang, L.Q. Chen, Phys. Stat. Sol. (b) 243 (2006), 1935-1841.
[16] Y.J. Hao, Q.Y. Lai, J.Z. Lu, X.Y. Ji, Ionics 13 (2007) 369.
[17] P. Kubiak, A. Garcia, M. Womes, L. Aldon, J. Olivier-Fourcade, P.E. Lippens, J.C. Jumas, J. Power Sources 119–121 (2003) 626.
[18] S.H. Huang, Z.Y. Wen, Z.H. Gu, X.J. Zhu, Electrochim. Acta 50 (2005) 4057.
[19] S.H. Huang, Z.Y. Wen, X.J. Zhu, Z.X. Lin, J. Power Sources 165 (2007) 408.
[20] T. Tabuchi, H. Yasuda, M. Yamachi, J. Power Sources 162 (2006) 813.
[21] J. Wolfenstine, J.L. Allen, J. Power Sources 180 (2008) 582.
[22] S.H. Huang, Z.Y. Wen, J.C. Zhang, Z.H. Gu, X.H. Xu, Solid State Ionics 177 (2006) 851.
[23] R. Dominko, M. Gaberscek, U. Bele, D. Mihailovic, J. Jamnik, J. Eur. Ceram. Soc. 27 (2007) 909.
[24] H. Liu, Y. Feng, K. Wang, J.Y. Xie, J. Phys. Chem. Solids 69 (2008) 2037.
[25] H.Y. Yu, X.F. Zhang, A.F. Jalbout, X.D. Yan, X.M. Pan, H.M. Xie, R.S. Wang, Electrochim. Acta 53 (2008) 4200.
[26] J.J. Huang, Z.Y. Jiang, Electrochim. Acta 53 (2008) 7756.
[27] L.X. Yang, L.J. Gao, J. Alloys Compd. 485 (2009) 93.
[28] A. Guerfi, S. Sevigny, M. Lagace, P. Hovington, K. Kinoshita, K. Zaghib, J. Power Sources 119–121 (2003) 89.
[29] A.Y. Shenouda, H.K. Liu, J. Power Sources 185 (2008) 1386.
[30] A.Y. Shenouda, K.R. Murali, J. Power Sources 176 (2008) 332.
[31] A.Y. Shenouda, Hua K. Liu, J. Alloys Compd. 477 (2009) 498.